

# CASCADE, neutron detectors for highest count rates in combination with ASIC/FPGA based readout electronics

Martin Klein<sup>a</sup>, Christian J. Schmidt<sup>b</sup>

<sup>a</sup>Physikalisches Institut, Universität Heidelberg, Germany

<sup>b</sup>Physikalisches Institut, Universität Heidelberg, Germany; currently at GSI Detector Laboratory, Darmstadt, Germany

---

## Abstract

The CASCADE detector system described herein is designed for high intensity neutron applications with high demands on the dynamical range, contrast as well as background. The detector front-end is a hybrid, solid converter gas detector using several gas electron multiplier (GEM) foils as charge transparent substrates to carry solid  $^{10}\text{B}$  layers. These coated GEMs are then stacked ("cascaded") one behind the other to cumulate the detection efficiency of every layer without losing position information. The use of GEM foils allows high count rates up to  $10^7$  n/cm<sup>2</sup>s. The well-defined neutron absorption locus inside the thin boron layer provides sub microsecond absolute time resolution, which opens the door towards new TOF applications. Because 96% isotopically enriched boron is available in large quantities in contrast to  $^3\text{He}$ ,  $^{10}\text{B}$ -converter based neutron detector technology is one of the very few technological alternatives to  $^3\text{He}$  in view of the imminent crisis in world-wide supply of  $^3\text{He}$ . Using GEM foils, the neutron detection bottleneck shifts to data read-out electronics and its bandwidth. The CASCADE detector uses an ASIC electronic front-end paired with an adaptable integrated FPGA data processing unit to provide high rate capacity and realtime event reconstruction.

**Keywords:** neutron detector,  $^{10}\text{B}$ , position sensitive, high count rate,  $^3\text{He}$  alternative, ASIC, integrated readout, FPGA

---

## 1. Introduction

Thermal and cold neutrons have kinetic energies of meV and below and therefore cannot be detected through recoil interactions in contrast to fast neutrons of MeV energies. They can only be detected through their interaction with matter in a nuclear reaction, thus resulting in a primary signal energy of order MeV with specific converters. There are only a few isotopes that can serve as a converter for the detection of such low energetic neutrons. These are the ones with a large cross-section for neutron capture as well as a suitable mechanism for energy release from the resulting excited nucleus. Some candidates like  $^3\text{He}$ ,  $^6\text{Li}$ ,  $^{10}\text{B}$  as well as  $^{235}\text{U}$  will generate heavy ionizing particles like alpha particles or even heavier ions. Others like  $^{111}\text{Cd}$ ,  $^{157}\text{Gd}$  or  $^{155}\text{Gd}$  will generate a  $\gamma$ -cascade, which in the case of Gd also yields low energetic conversion electrons.

For thermal neutron detection in general, gas-detectors with  $^3\text{He}$  as gaseous converter were favored whenever high sensitivity to neutrons paired with low sensitivity to gamma radiation was the criterion of design. Among the few neutron-converting isotopes with reasonably high conversion cross-section,  $^3\text{He}$  had proven to be a stable, chemically inactive and reliable converter. Also, its (n, p) reaction provides for moderately short ionizing tracks and correspondingly good spatial resolution. However, right from the start, these detectors need to be operated at high gas pressure in order to combine detection efficiency requirements for thermal and cold neutrons with acceptable time resolution. The typical operating pressure of 10 bar and beyond is o.k. for proportional counter tubes [1]. For two dimensional wire chambers of reasonable size, however, such

operating pressure poses a serious mechanical challenge [2][3].

New, high-intensity modern neutron sources as the US-American SNS [4] as well as J-PARC in Japan [5] came into operation recently. In the strive to match detection needs on instruments at spallation neutron sources to the thousand fold higher instantaneous flux prospected, likewise the competitive drive at existing neutron sources to improve and match performance to these modern sources [6], the  $^3\text{He}$  detector - and any other neutron detector using a gaseous converter together with combined gas amplification and wire readout - reveals its major disadvantage: Due to the comparatively slow drift velocity of ions, this detector technology is limited in detection rate to some 20 kHz at any point. The corresponding dead time of the pixel can be accounted to space charge effects. It depends upon the drift time of ions to be removed at the cathode and thus upon the distance and the drift velocity and with it the operating pressure as well as the counting gas itself. Furthermore for gaseous converters, most of these parameters are predetermined by other criteria like the detection efficiency, so there is very little room for optimization.

Additionally with  $^3\text{He}$ , an entirely new problem has come up during the last year, namely a severe crisis of the availability of  $^3\text{He}$  itself [7]. Global disarmament of thermonuclear weapons, in which formerly  $^3\text{He}$  was generated through the decay of Tritium, severely reduced the sources of this precious gas and made it entirely unavailable for scientific applications.

This unexpected situation even accentuated the need for alternatives to  $^3\text{He}$  based detector technologies. We are convinced, that CASCADE has developed to be a real technologi-

cal alternative to  $^3\text{He}$  based neutron detectors.

In order to overcome the limitations of  $^3\text{He}$  based neutron detectors with focus on very high count rate capability paired with high dynamical range as well as very low background sensitivity, the CASCADE neutron detector system described herein was developed. It is based on a stack of many thin boron layers to absorb most thermal neutrons and to efficiently detect the escaping nuclear reaction products inside a gas detector while being insensitive to  $\gamma$ -background at the same time. Use of GEM foils [8] allows high count rates up to 10 MHz/cm<sup>2</sup> [9] and leads to the usage of highly integrated readout electronics.

## 2. Neutron detection with solid converters

In general, solid neutron converting materials have the advantage that a large absorption cross-section can be realized over very short distances. In the ideal case, the converting material itself would act as an active electronic readout device for the secondary charges produced in the same device by the neutron nuclear reaction products. Results on small boron based semiconductor devices can be found in [12][13][14]. However, the few existing neutron converting materials are mostly passive and do not allow for the direct detection of secondary charges or excitations generated by neutron nuclear reaction products. Converters are sensitive only in the thin outermost layer, from which the energetic reaction fragments could still escape. So the absorption depth by itself is of little help.

To judge the single layer detection efficiency the penetration depth  $R$  of the charged fragments in the particular converter in comparison to its thermal neutron absorption length  $\lambda_n$  has to be considered.  $^{157}\text{Gd}$  shows the best ratio of  $R/\lambda_n = 9.2$ , followed by  $^6\text{Li}$  with 0.57 and  $^{10}\text{B}$  with 0.16. This quality led e. g. to the proposal of the  $^{157}\text{Gd}/\text{CsI}$  based low-pressure MSGC detector at HMI [15]. Its detection scheme is based upon the  $^{157}\text{Gd}(n, \gamma)^{158}\text{Gd}^*$  conversion reaction, where the low energetic conversion electrons with 29-182 keV have to be distinguished from any compton scattered background depositing similar energies.

Other solutions have led to concepts, where the solid converter is diluted to maximize its surface either in a matrix of scintillating, translucent material or, by some other means sandwiched in active detector material, suitable for the detection of charges. This could e.g. be silicon or, alternatively, a gas detector as is the case of the CASCADE detector. The primarily favored scintillator alternative [17] suffers from a considerable sensitivity to gamma radiation, which must be accounted to the large amount of sensitive material and the resulting limited count-rate dynamic range. Silicon [16], the boron based semiconductor devices as well as boron enriched MCP's [18] are restricted to mostly fixed, micro-scale pixel sizes. The motivation for the development of the CASCADE detector concept was, to combine and exploit the advantages of gas detectors with the well-defined locus of conversion of solid neutron converting materials.

### 2.1. $^{10}\text{B}$ solid converters

If the detector concept is based on a stack of several thin converting layers to absorb most of the thermal neutrons and

to efficiently detect the escaping nuclear reaction products inside a gas detector, then the  $R/\lambda_n$ -criterion would be weaker, giving room to choose other materials and to optimize several criteria at once. For this reason  $^{10}\text{B}$  was chosen as converting material for the CASCADE detector. It proved to be the best compromise among a variety of criteria:

- $^{10}\text{B}(n, \alpha)^7\text{Li}$  with  $Q = 2.8$  MeV yields a comfortable amount of energy.
- $^{10}\text{B}$  has a considerable capture cross-section for thermal neutrons of 3836 barn.
- The range of fragmentation products in typical counting gas is on the order of a few mm at atmospheric pressure. It sets the range for spatial resolution and was determined to 2.6 mm (FWHM) in our setup (see fig. 11).
- Yet, their range in amorphous solid boron is considerable: for a single isotopically pure layer the corresponding probability of leaving the bulk to be registered results in an overall detection efficiency of 5% for thermal neutrons (1.8 Å) [19][20]. For cold neutrons (5 Å) the single layer efficiency is about 12% and for ultra-cold neutrons up to 90% efficiency can be reached.
- Boron is chemically inert, non hygroscopic as well as electrically very high resistive ( $1.8 \times 10^6 \Omega\text{cm}$ ). No protective passivation layers need to be added. 96% isotopically enriched  $^{10}\text{B}$  is available in large quantities.
- Finally, the low atomic number guarantees negligible sensitivity to gamma radiation.

### 2.2. The boron conversion pulse-height spectrum

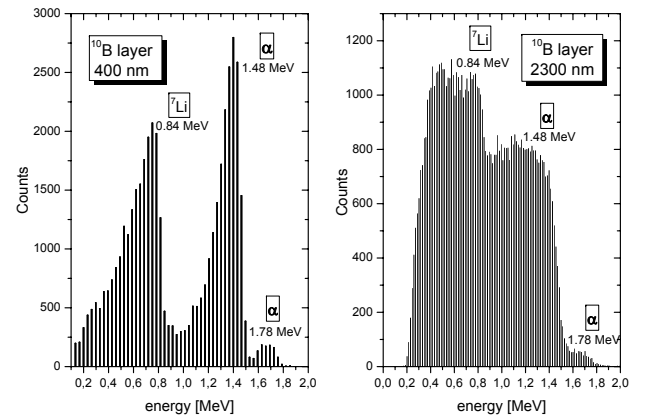


Figure 1: Pulse height spectra for two different boron layers measured at moderated  $^{252}\text{Cf}$ -lab source. A layer thickness of about 400 nm (left figure), which is much less than the penetration depth of the  $\alpha$ - and  $^7\text{Li}$ -particle in boron, shows clearly the higher energetic  $\alpha$ -peak broadened down to zero. The lower energetic peak of  $^7\text{Li}$  is added on top of the tail of the  $\alpha$ -spectrum. If the thickness is comparable to the particles' penetration depth in boron (right figure), then the spectra of the mono-energetic lines are entirely smeared out to 0, here measured with a particularly high threshold setting. For the CASCADE a boron thickness of about 1.2  $\mu\text{m}$  is used implicating an intermediate shape of the spectrum.

Neutron absorption inside the solid boron layer along the incident neutron direction results in an exponentially falling density distribution of the charged fragments. They, namely the  $\alpha$ -particle and the  ${}^7\text{Li}$ -nuclei, start in opposite direction from these conversion points, so that only one of the two particles can reach the gas volume at once while the other particle hits the support foil. At the same time when traversing the solid layer to reach the counting gas, the particle will deposit already some fraction of its energy inside the boron layer, which will be not available any more for primary ionization inside the gas itself. Furthermore, because of the particles limited range of 1-3  $\mu\text{m}$  within the boron itself and depending from the thickness of the boron layer, there exists even a small solid angle, within no particle will reach the counting gas and therefore will be lost for counting. As a result, the final pulse-height spectrum of a solid layer shows a continuous energy distribution starting from the maximum energy ( $\alpha$  at 1.78 MeV,  ${}^7\text{Li}$  at 1.01 MeV) reaching down to zero and thereby reflecting the thickness of the layer (see fig. 1).

A much more detailed discussion of the aspects of thin solid boron layers can be found in [19] and was worked out for the CASCADE detector in [20].

As a final remark, the interpretation of pulse height spectra will result even more complicated, if the depth of counting gas is chosen below the particles' penetration depth in the gas, as it is the case in our setup with a typical gap of only 2 mm. Intensity from higher pulse height channels then appears shifted to lower channels. The spectrum suffers from a further convolution, when read out through a segmented readout structure with a pitch smaller than the particles' penetration depth. However, for the efficiency of neutron detection only the fraction of signals above noise and the background ( $\gamma$ -rays) level is relevant.

### 3. The CASCADE detector concept

Boron coated ionization cells or Geiger-Mueller tubes are known for neutron detection ever since neutron sources were available. They are simple and robust but unfortunately limited to two boron layers' detection efficiency. Further enhancement is feasible only by adding more boron layers. For a position sensitive area detector, however, such additional layers must be transparent for charge while opaque for neutrons. This apparent contradiction can be resolved when employing gas electron multiplier (GEM) foils invented and developed by Fabio Sauli at CERN in 1997 [8]. GEMs are micro-structured, flexible foils of a 50  $\mu\text{m}$  thick Kapton substrate, sandwiched between 5  $\mu\text{m}$  thick copper claddings on either side. The foil is micro-structured with a regular hexagonal grid of 50  $\mu\text{m}$  diameter holes at a spacing of 140  $\mu\text{m}$ . They are nowadays available in sizes up to 40cm  $\times$  70cm [10]. Depending upon the potentials applied to the two copper claddings on top and bottom, every hole serves as an electrostatic lens, which allows to guide and image charge from one side of the foil through the holes to the other side without loss of in-plane position information. With larger potential differences, the field strength in the holes can be made strong enough to cause charge amplification.

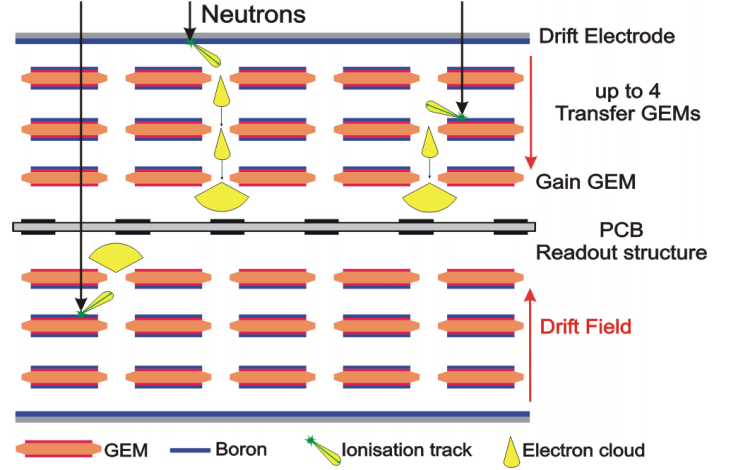


Figure 2: Schematic view of the CASCADE detector concept. Many GEM-foils stacked behind each other are coated with thin layers of  ${}^{10}\text{B}$ , absorbing incoming neutrons and converting them into charged particles as e.g.  $\alpha$ -particles, which deposit most of their energy in the gas filled gap between two GEM-foils. Charge transfer to the readout structure is accomplished by several Transfer-GEM-foils and one Gain-GEM-foil. The symmetric foil arrangement around the common readout structure reduces high voltage levels that need to be handled.

For the CASCADE detector, several of these GEM-foils are used as charge transparent substrates to carry boron layers (see fig. 2). These coated GEM-foils are then stacked ("cascaded") one behind the other to cumulate the detection efficiency of every layer without loosing the lateral position information of the neutron absorption and conversion locus. The charges generated by the fragmentation products in the gas spacing (typical gap distance is 2 mm) between successive GEM-foils are channeled through the GEM-foils to one common readout structure. These Transfer-GEM-foils are operated with an effective gas gain of 1 while the last GEM-foil (Gain-GEM) is operated with a moderate gain of 10-30 in order to raise signals comfortably above the noise level of the electronics and readout structure we employed.

As a result, this concept provides a neutron detection scheme, where each step can be optimized independently with different goals:

- Neutrons are converted into charged particles by multiple solid converter layers.
- The charged fragmentation products deposit their energy in any suitable, cheap counting gas at e.g. atmospheric pressure. Pressure and gas composition can be optimized without impairing neutron detection efficiency.
- Cheap counting gas allows a constant exchange of gas that removes all contaminants inside the detector. Ageing effects, potentially causing a decrease in the detection efficiency due to chemical reactions under high-count rates are reduced considerably and allow long-term stability. Operation of gas detectors in a constant purging mode may be novel to the field of thermal neutron detection, it is however a well-established and widely employed technique in high energy and nuclear physics.

- The overall signal height is set to a convenient level by the potential difference on the last GEM, a near noiseless amplifier of variable gain. Further this micro-structured device is responsible for the inherent rate capability of 10 MHz/cm<sup>2</sup> [9].
- Finally, clouds of charge rain onto an adequate signal readout structure. Signal readout is independent of signal amplification, which makes it feasible to adapt pixel size and shape, the readout geometry (one- or two-dimensional) or even the readout strategy (single pixel readout, 2D-coincidence correlation readout) to the particular needs of the neutron scattering instruments.

As an example, the actual detector design with 200mm × 200mm sensitive area is targeted for operation at ambient pressure so that no enclosing pressure tank is necessary (see fig. 8). In consequence, it can be constructed as a lightweight detector with a minimized frame of blind area measuring 10 mm around the sensitive area. Even larger sizes are feasible now [10]. Thus, several detector modules can be tiled modularly to cover larger solid angles. Alternatively, if very high spatial resolution is to be achieved, a moderate 2-3 bar overpressure in combination with the right choice of counting-gas, allows an enhancement down to 1 mm. For demonstration we have build a pressure chamber for the actual 200mm × 200mm CASCADE detector. The detector was equipped with a 2D readout structure (x- and y-stripes of 1 mm pitch) and tested in front of our moderated <sup>252</sup>Cf-lab source. Figure 3 shows the measured position resolution in dependency of the absolute counting gas pressure.

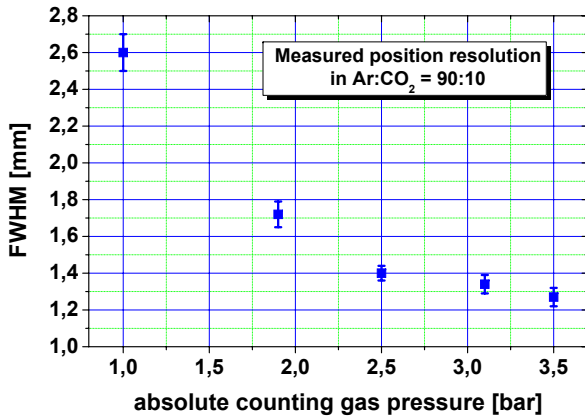


Figure 3: Position resolution for the actual 200mm × 200mm CASCADE detector in dependency of the absolute counting gas pressure. Because of the low neutron intensity available at the <sup>252</sup>Cf-source, position resolution was determined through a fit to the measured edge-spread-function.

### 3.1. Thermal neutron detection efficiency

To get more than one boron layers' efficiency, the CASCADE detector concept accumulates the single layer efficiency of many thin boron layers stacked behind each other. Adding more and more boron layers does however not lead to a linear

increase in detection efficiency but rather to exponential saturation. This saturation effect sets a natural scale for the accumulated absorption at  $(1 - 1/e) \approx 63\%$ . Adding more and more layers beyond this natural limit does not lead to a significant increase of detection efficiency, but increases drastically the effort and the costs. Furthermore it raises the absolute value of high voltage potentials needed along the stack of GEM foils to generate the needed drift field strength over the entire stack.

So addressing an accumulated absorption of about 70% for thermal neutrons (1.8 Å) will result in an absolute neutron detection efficiency of about 50% due to the geometrical losses of charged particles inside the solid boron layer as discussed in section 2.2. 50% detection efficiency can be reached using 20 layers of <sup>10</sup>B, coated onto both sides of 10 GEM-foils. The optimum <sup>10</sup>B layer thickness is in this case found to be around 1.2 - 1.4 μm. Operation of a cascade of 10 GEM foils necessitates high voltage in the range of 6-7 kV, which is not easy to handle in our compact design. Instead, a symmetrical setup of GEM-foils around one common readout structure as shown in figure 2 was chosen to reduce high voltage levels by a factor of 2 to an absolute value of 3-3.5 kV. This configuration appeared to work stable and reliable.

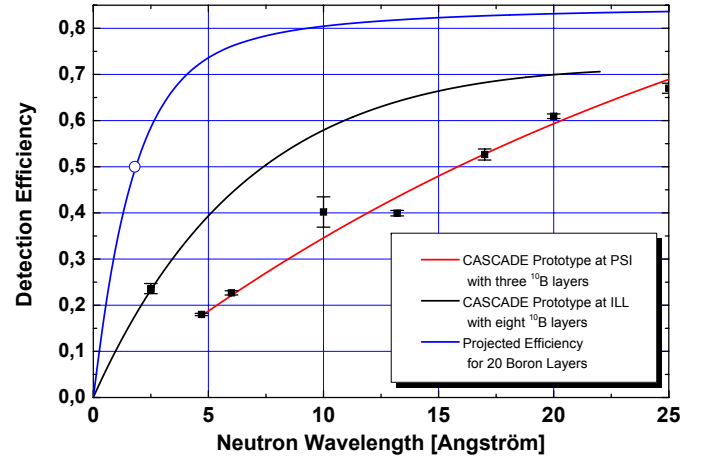


Figure 4: Absolute detection efficiency for thermal neutrons determined for two different detector prototypes. Data points were measured, the lines mark extrapolations to other wavelengths as well as for 20 Boron layers. The absolute detection efficiency was determined using calibrated <sup>3</sup>He tubes. Measurements at PSI were performed at the SANS instrument whereas at ILL the beams at instruments CT2 and PF1-A were used.

Up until now, several detector prototypes equipped with up to 8 boron layers coated on GEMs and drift electrodes were build and successfully tested. The measured detection efficiencies proved to be in good agreement with theoretical calculations (see fig. 4). In these detectors the GEM foils were coated only single sided. Small GEM foils of 50mm × 50mm size coated on both sides have already been tested successfully. Several larger size GEM-foils when coated on both sides up until now still showed a leakage current. The coating process is under further development to address this problem. With ten singly coated GEM-foils, an overall detection efficiency of 35% (1.8 Å) and 55% (5 Å) can be reached.

### 3.2. Gamma sensitivity

The CASCADE detector, as a gas detector, exposes very little mass to the neutron and gamma fluxes. Further, it is entirely constructed of low Z materials, including the neutron converter  $^{10}\text{B}$ . These properties make it inherently insensitive to gamma radiation. Finally the insensitivity is accentuated by the enormous difference in ionization density of a fast electron from compton scattering creates in the counting gas as opposed to an alpha particle from neutron conversion. In practice, the free path of an energetic electron in the counting gas is geometrically limited to a few mm (the typical gap distance between two GEM-foils being 2 mm, the pixel-readout size  $1.56\text{mm} \times 1.56\text{mm}$ ), so that such electron signals will remain unregistered in individual channels.

We tested a  $200\text{mm} \times 200\text{mm}$  sensitive detector prototype in the direct beam of the former instrument PF1-A at the ILL, which provided a cold neutron beam with around  $10^9 \text{ n/cm}^2\text{s}$  on a beam cross section of  $50\text{mm} \times 70\text{mm}$ . The entire detector area was covered with cadmium to absorb all incoming neutrons and resulting in a tremendous amount of gamma-ray cascades. An integral background rate of 4 Hz was measured over the entire detector area.

### 3.3. Mechanical design

Much care was taken in the exact choice of materials avoiding hydrogen, which generates incoherent background. Also the outgasing properties of all materials have been taken into account in order to avoid ageing effects, typical at the high intensities targeted. Concerning ageing, the knowledge base from high-energy physics gas detector construction was exploited for a rugged concept.

## 4. Rate capability compatible with flux at spallation neutron sources

### 4.1. Inherent front-end rate capability

Micro structured GEM-foils introduce an inherently high rate capability. GEM-foils have been evaluated by CERN for rates up to  $10 \text{ MHz/cm}^2$  [9]. Using a CASCADE prototype this could be confirmed for neutron detection in count mode up to at least  $4 \text{ MHz/cm}^2$ , where our measurements were clearly limited through the bandwidth of the particular pre-amplifiers employed. Figure 5 shows a time of flight spectrum measured at PF1-A (ILL). The raw data plotted are not dead time corrected and purely show the measured instantaneous detection rate on a logarithmic scale. It gives a lower limit for the dynamic range of at least 50000. The structured background beyond 10 ms flight time can be attributed to leaks in the particular chopper disk employed for the measurement (a Gd-painted disc).

During these test experiments, detector robustness was also explored. To this end the detector was exposed to a neutron beam that caused an estimated  $600 \text{ MHz/cm}^2$  neutron conversion rate on an area of  $2.2 \text{ cm}^2$ . Individual neutron pulses could definitely not be resolved at these rates. After 2.5 hours of continuous irradiation under these conditions, the neutron flux

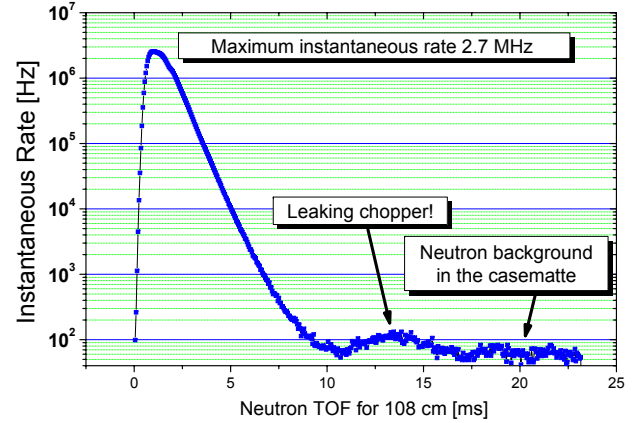


Figure 5: TOF measurement realized in the direct beam of PF1 A (ILL) with eight cascaded layers of  $^{10}\text{B}$  and reading out with a single pre-amp one single stripe of  $1 \text{ cm}^2$ . A maximum of 4 MHz instantaneous rate was measured within these experiments.

was again greatly reduced and the detector immediately resumed normal operation again. Successive time of flight measurements showed no degradation of detector performance after this experiment.

### 4.2. System readout bandwidth

With the typical high rates bottleneck in the detector front end resolved, the bandwidth of readout electronics immediately imposed the next. In response to this problem, we decided to pioneer the transfer of highly integrated ASIC-based readout technology from high-energy physics into the field of neutron instrumentation. But in case of a position sensitive detector system the detection device itself and its readout electronics have to be matched very carefully, because the quality of interplay proves essential for system performance.

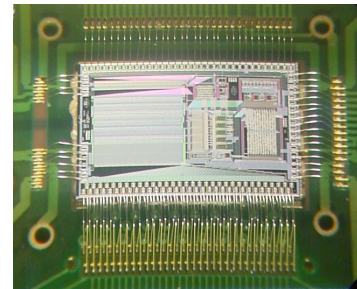


Figure 6: Photograph of the CIPix ASIC. Clearly visible are the bond wires at the bottom that feed the analogue input signals into 64 pre-amp channels. The chip measures  $4.1\text{mm} \times 6.7\text{mm}$ .

For the CASCADE detector, the CIPix ASIC (see fig. 6) is employed as readout device. This chip was originally developed by the Heidelberg ASIC lab in 2000 for the DESY H1 experiment [21]. A single chip integrates 64 channels of a low noise charge sensitive preamplifier followed with a shaper and discriminator (see fig. 7). The amplified and shaped input signals are digitized by an AC-coupled comparator with configurable polarity sampled at a clock rate of 10 MHz. Each chan-



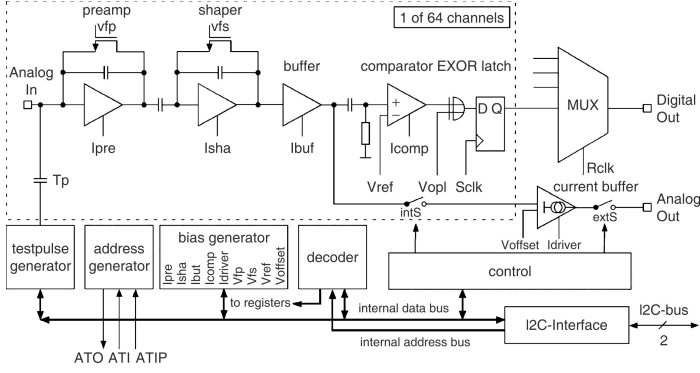


Figure 7: Schematic diagram of the CIPix ASIC. A single chip provides 64 independent analogue channels comprising pre-amp, shaper and programmable comparator, the latter being sampled and processed at a rate of 10 MHz.

nel can accept statistical data at a rate of about 330 kHz at 10% dead time, resulting in an immediate specification for the individual pixel rate capability of the same size, no matter how the pixel is read out. The digitized states of every comparator are multiplexed by 4 onto 16 digital outputs with a readout clock of 40 MHz, synchronous to the sampling clock. The bias settings and various other parameters are programmable and can be accessed via an I<sup>2</sup>C-bus. For diagnostic purposes, the analogue output of any shaper may be switched to one output monitoring channel. Thus, for one selectable channel, the full analogue behavior may be observed. Furthermore, the chip is equipped with a programable internal test-pulse generator that allows to inject test-pulses into any given channel.

Two-dimensional readout of large detector areas is realized through a correlation of signals in time from coordinates  $x$  and  $y$ , using several CIPix chips. In discussion on the overall detector readout bandwidth one has to recognize, that the architecture of typical front-end ASICs (developed so far mostly for high energy physics experiments as the herein used CIPix chip) is based on the fact, that an external pace giving clock from the collider driven experiment is always available (so called bunch clock). This scheme is used to synchronize and adapt the readout bandwidth to the readout rate needed.

In the typical neutron application, no external trigger is available. On the contrary, individual neutron events are entirely uncorrelated. Instantaneous event rates show a poisson distribution for the time of arrival within the neutron detector. So available externally synchronized front-end ASICs can be used for neutron detection, but they are rate-limited because of their regular readout pace. In consequence the useful readout bandwidth for neutron detection is typically 10 times less than the clock driven electronics does provide, when dead times of 10% are accepted. Using the available CIPix chip running at 10 MHz, the overall detector readout bandwidth is therefore limited today to 1 MHz at 10% dead time. It is limited by the minimum time-binning width of the chip giving a correlation time of 100 ns for 2D position resolution by coincidence correlation. Higher overall detector rate capability of course can be achieved through segmentation into several independent regions of position correlation at the expense of additional elec-

tronics. Clearly, detector overall rate capability directly scales with the amount of electronics it is equipped with.

## 5. The actual CASCADE neutron detector with 200mm × 200mm sensitive area

The CASCADE detector system is conceived as a standalone, position sensitive neutron detection device, where the entire electronic readout (front-end ASICs and DAQ system with local memory) is directly mounted onto the back of the device (see fig. 8). Once externally configured, the DAQ system performs predetermined measurements. The entire measurement and data acquisition runs locally on the detector module, asynchronous to any external instrument control and data storage system.

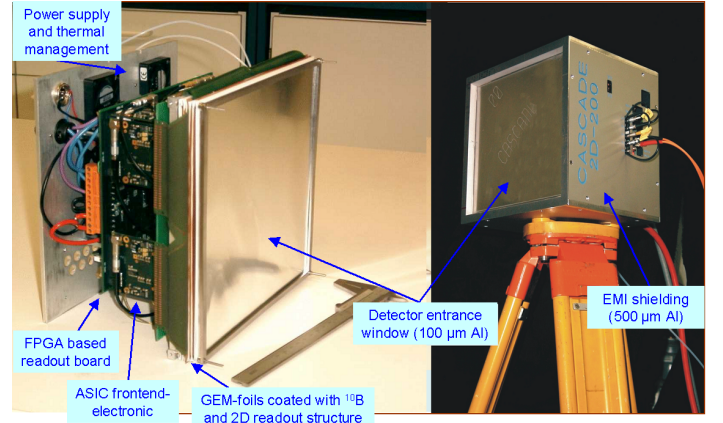


Figure 8: The actual CASCADE detector module of size 200mm × 200mm.

### 5.1. 2D signal readout

The sensitive area of 200mm × 200mm is read out on 128 independent channels for each coordinate, resulting in an overall image of  $2^7 \times 2^7 = 16384$  pixel in 2D-coincident correlation mode. Two-dimensional signal readout is realized through a charge-sharing scheme similar to that shown in [11]. A cloud of charges, when raining onto the readout structure, will be collected by electrodes corresponding to both dimensions  $x$  and  $y$ . Thus, simultaneous registration of signals on  $x$ - and  $y$ -readout channels reveal the detection of a neutron at the corresponding  $(x, y)$  coordinates. Much effort was invested to optimize the readout structure for minimum capacitance while maximizing the probability that electrodes of both coordinates will be hit.

A two-dimensional radiography using cold neutrons at FZ-Jülich is depicted in figure 9. Here, a block of polyethylene at the beam exit was used to generate an isotropic source of neutrons to illuminate the entire detector, which was set up on one side of the beam-line. Various items, a dispenser for scotch tape as well as a water flow indicator (upper left) and an old fashioned computer mouse (upper right) were placed directly on the entrance window. Their images can clearly be recognized.

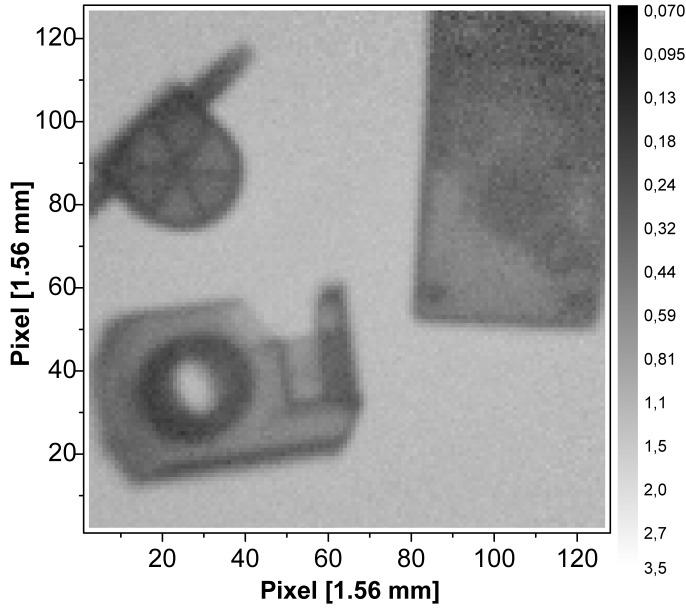


Figure 9: Radiography measured with cold neutrons at FZ-Jülich.

### 5.2. Spatial resolution and the point spread function of the CASCADE detector

One important characteristic of an area detector is its spatial resolution, usually defined as the FWHM of a peak that was generated by an infinitely narrow beam ( $\delta$ -function response). In particular for neutron scattering however, not just the width, but the entire  $\delta$ -function response curve, usually termed the point spread function (PSF), is of great interest. In particular, as neutron data is very often analyzed on a logarithmic scale (ratios of intensity are the focus), the baseline halo intensity of such a PSF is of principle interest.

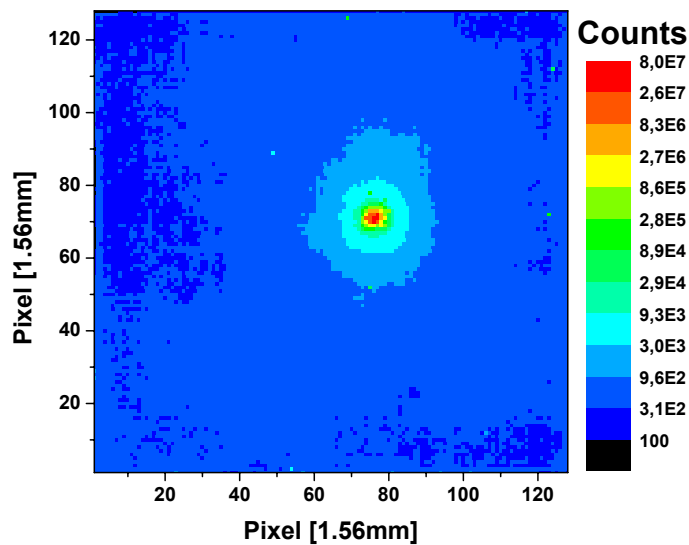


Figure 10: Two-dimensional PSF measured at the former instrument EKN at FZ-Jülich using a cold neutron beam of 0.57 mm diameter. Data are plotted on a logarithmic scale.

For the CASCADE detector the two-dimensional PSF was measured using a thin, collimated neutron beam of 0.57 mm diameter. The detector response is shown in figure 10 on a logarithmic scale. The profile along the y-direction across the peak of the PSF was extracted and is shown in figure 11. It reveals a width of  $(2.6 \pm 0.1)$  mm (FWHM) for the peak and a halo-intensity starting at a level of 200 ppm and falling rapidly with radial distance from the peak. The remaining halo intensity may be attributed to a general neutron background, cross scattered neutrons as well as some neutrons incoherently scattered by hydrogen content in the GEM substrate.

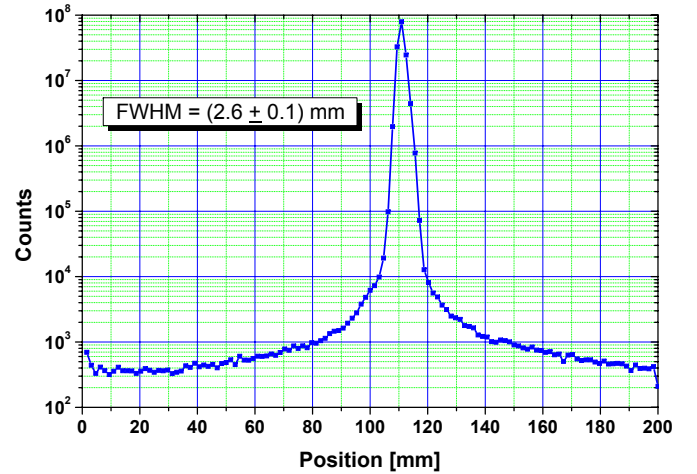


Figure 11: Profile along the y-direction across the PSF extracted from figure 10. Position resolution can be determined to  $(2.6 \pm 0.1)$  mm (FWHM). The detector is operated with a counting gas mixture of Ar/CO<sub>2</sub> (90%/10%) at ambient gas pressure.

### 5.3. Real time DAQ

Ultra high bandwidth data acquisition systems have been and are still pioneered by high energy physics, developing analogue front-end readout chips and using modern Field-Programmable-Gate-Array (FPGA) technology. Here, primarily rapid data reduction through complicated event selection algorithms and hardware are targeted (first and second level trigger systems). For neutron applications on the other side, high statistics and very little event selection are essential. The entire data acquisition system needs to be of comparable broad bandwidth, which is the core technological challenge.

For the actual 200mm  $\times$  200mm CASCADE detectors an FPGA based readout board (see fig. 12) was developed, which is directly mounted onto the back of the device (see fig. 8). It collects the data output of up to five CIPix chips simultaneously (see fig. 13). Because the ASICs generate data continuously at 10 MHz on each channel without zero-suppression, they produce a huge data load of 3.2 GBit/sec, that can only be handled in real time by massive parallel processing.

Therefore, inside the FPGA a real time event reconstruction algorithm evaluates the incoming data from the readout structure together with the time stamp information  $t$  synchronized by an external chopper to one neutron event  $(x, y, t)$ . Furthermore

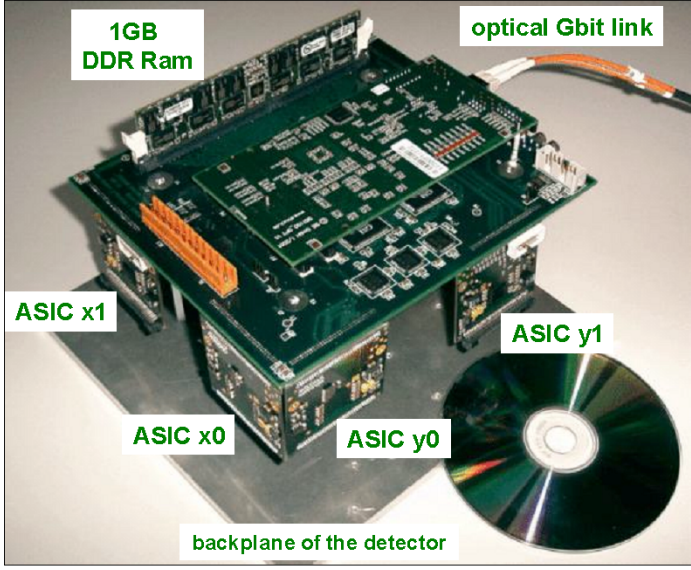


Figure 12: Photograph of the FPGA-based DAQ board developed to read out and to control up to five CIPix chips simultaneously. It realizes the real time event reconstruction of neutron events occurring in the detector and registered by the ASIC readout chips. Equipped with local memory up to 1 GB it allows to run the entire measurement and data acquisition locally on the detector module, asynchronous to any external instrument control and data storage system.

the FPGA's firmware manages the on-board memory to realize freely configurable histogram counters. An overall number of 256 million data counters together with 4 million monitoring counters may be employed with a depth of 32 bit each. Fast logical inputs can be used to trigger time of flight measurements externally. The 256 million histogram channels could for example be configured to realize a three dimensional histogram containing a time of flight (TOF) spectrum for every single one of the 16 thousand pixels simultaneously [22]. Meanwhile, the monitoring histogram can be set to cumulate and monitor the data in much coarser spatial or time resolution, but with higher statistics. This channel allows to quickly and on-line retrieve an overview if the measurement is operating right, without in-

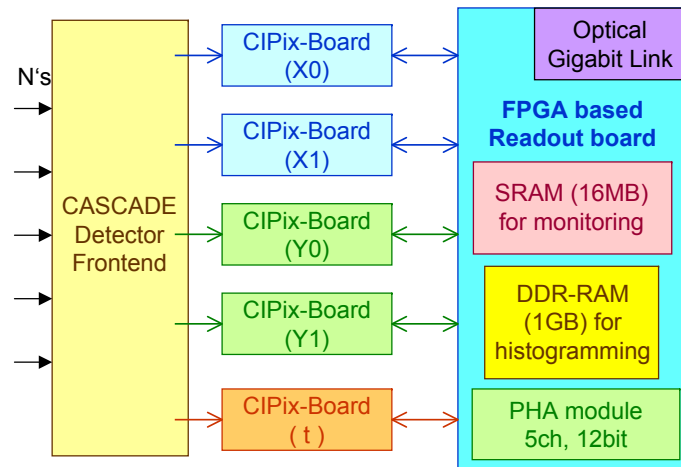


Figure 13: Schematic of the real time DAQ system.

terfering the measurement itself. Data collection is performed simultaneously and independently at high resolution into the on board data histogram.

Communication with the detector module is realized through a fiber optical link, which decouples the system galvanically. It serves on one hand to configure the module through a few user accessible registers. On the other hand it provides a high bandwidth data link, which serves to download the histograms of measurements, the module has acquired. Finally, also list-mode data can be taken and read out as one possible configuration.

For direct diagnostic purposes, any selected readout channel of the CIPix chips can be investigated measuring its pulse height spectrum. To this end an additional ADC sub-module is mounted onto the FPGA board providing five 12-bit ADC's sampling at 40 MHz each. Peak heights are digitally analyzed prior to histogramming the corresponding pulse height spectrum.

#### 5.4. Real time event reconstruction

The immense data load of 3.2 GBit/sec coming from up to 5 CIPix chips is handled in real time inside the FPGA's firmware by a massive parallel processing algorithm. Further, the firmware incorporates and addresses the special properties and particular gas detector physics of the CASCADE detector. It filters and extracts the neutron conversion events, assigns these a particular (x, y, t)-coordinate and finally realizes the filling of pre configured histograms. The firmware is programmed in the hardware description language VHDL. Its flow diagram is depicted in figure 14, the blocks of which are referred to in the following.

First, entity *Demux* synchronizes the incoming CIPix signals to the internal FPGA's global clock. After synchronization, the CIPix signals will be demultiplexed 1:4 and the *CIPix Data Valid* signal will be generated for further processing.

The entity *Readout Structure Mapping* sorts the incoming CIPix signals, encoding the particular 2D readout structure employed, into a linear data vector. Furthermore, by use of the *Mask Registers*, further processing of any desired data channel (stripe) may be masked out and inhibited, which may be helpful in case of noisy or defect channels.

Development work on the firmware needs to be proved repeatedly. To facilitate the analysis of the firmware's correct logical functionality after compilation as well as the correct timing behavior, the *Simulator* block was added, which generates artificial data and mimics CIPix and detector operation with a freely programmable time pattern. This simulator may be multiplexed into the data stream within the final firmware under test. The non statistical, pre-determined data serves to test the data pipeline, event reconstruction, data histogramming and communication with external hardware and software as it is to be processed in a deterministic way. Even very special, rare data structures or even the outcome of non physical data input may then be studied.

The block *List-Mode Data Fifo* implements a data fifo of 4096 elements depth to store CIPix data vectors (64 bit for each CIPix chip) as they flow in time slices of 100 ns inside



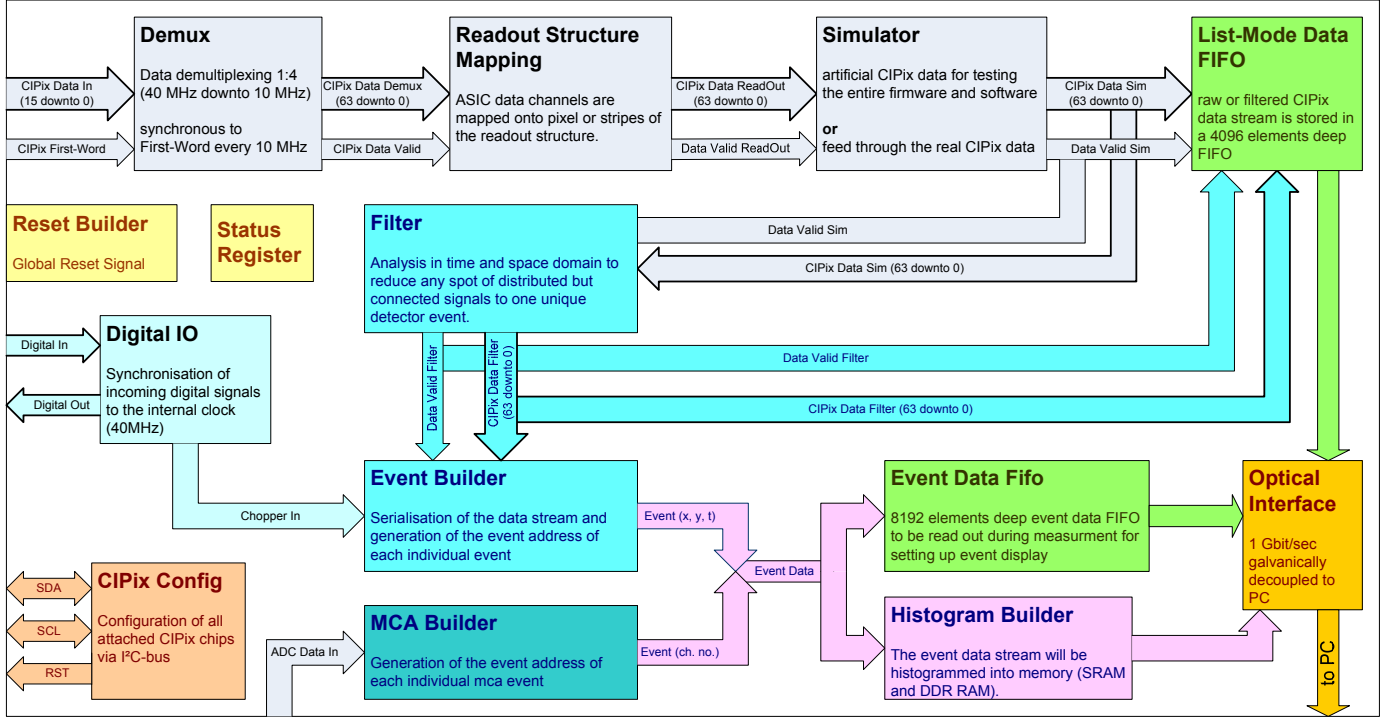


Figure 14: Schematic of the data flow inside the FPGA's internal firmware.

the firmware. This fifo serves to store alternatively either raw CIPix data directly after demultiplexing or processed data after event reconstruction. The former is used for testing, the latter may be employed for operational data acquisition if histogramming is not desired.

The entity Filter is responsible for the identification of individual neutron events out of the data stream. On the input it receives the data vectors of all channels for both spatial coordinates at the sampling rate of 10 MHz. First of all a coincidence analysis of the data is done to detect the occurrence sudden common mode signal distortions due to electromagnetic interference EMI. For EMI identification, the simultaneous firing of channels at the corners of the readout structure is detected and an analysis performed on how many channels over all are firing simultaneously. The data stream is then nulled for the relevant clock cycle.

Any real neutron event will reveal itself as a signal in one or more neighboring channels and over one or more connected time bins. Thus, in a second step towards identifying neutron events, this entity does an analysis in the time and space domain to reduce any spot of distributed but connected signals to one unique detector event. In the case of ambiguities as for example due to simultaneous disconnected multi-hits the data slice is rejected. Accepted signals are single stripe, 2 neighboring stripes or 3 neighboring stripes and signals up to 4 time cycles long (400 ns). Two spots of connected signals can be identified as two individual neutron events as long as they do not begin within the same time slice. Ambiguous signals or spots in the time-space domain, which cannot be assigned to an individual neutron event, are filtered out.

A set of counters is used to monitor filter activity by counting signals successfully reduced to neutron events, signals that could not be correlated to the other coordinate or such that had to be filtered out as the signal spot occurred too broad in the space or time domain to be attributed to a single neutron. These counters provide an online analysis on the statistics of signals in space and time, that occur in the detector. Optionally, signal filtering and reduction may be switched off entirely, so that the raw data are transferred for histogramming.

The Event Builder is the master entity of the entire firmware. It starts and runs a measurement. It is responsible for the generation of the event address for each individual event indicated in the data stream by the Filter entity. The parallel incoming data stream is buffered, analyzed and serialized into a sequential event data stream of spatial coordinate and time stamp (x, y, t), that can be histogrammed now.

The Histogram Builder receives the serialized event data stream from Event Builder to be histogrammed into the local memory (SRAM and DDR-RAM).

### 5.5. Very high TOF-resolution towards new TOF applications

A fifth CIPix chip, not needed for spatial readout, may be employed for coincident readout of all GEM-foils in the stack. These data can be evaluated in parallel to identify, in which boron layer the absorption of the neutron took place. This feature was developed for an application where time resolution was of particular interest. By its use, complete TOF spectra for each boron layer and each pixel of the readout structure are generated. This allows to realize very high time of flight resolution down to 100 ns as the locus of conversion may be determined to

within the thickness of a boron layer. It opens the door towards new TOF applications such as the MIEZE technique [23].

MIEZE is a special Neutron Resonance Spin-Echo method (NRSE) used for high resolution, quasielastic neutron scattering. Because the MIEZE technique results in a very fast modulated neutron intensity with modulation frequencies from 10 kHz up to the MHz regime, it requires high intrinsic detector time resolution. In a first test experiment [24] we could successfully measure a fast modulated neutron beam with intensity varying at a frequency of up to 654 kHz. Through additional direct readout of the coated GEM foils, the full contrast of the intensity modulation absorbed by 4 boron layers could be detected, which demonstrates time of flight resolution down to 100 ns.

## 6. Outlook: the n-XYTER, a dedicated neutron detection ASIC

Neutron applications rather demand a readout architecture, that is entirely data driven and where every readout channel is supplied with its individual asynchronous discriminator and time-stamp. Statistical rate fluctuations may then be buffered so that only the mean signal rate needs to be covered by the readout bandwidth. Maximum instantaneous rates are then limited by analogue pile-up and may be a factor of ten times higher than the mean rate.

For this reason, an entirely data driven front-end ASIC, dedicated to neutron detection and other statistical signals, was developed within the EU FP-6 initiative NMI3 (DETNI) for the particular use in the CASCADE detector [25] and two other high rates neutron detectors. In future the CIPix chip for the CASCADE detector will find replacement by this dedicated neutron readout ASIC chip n-XYTER (neutron- X, Y, Time and Energy Readout) to achieve minimum 10 MHz count rate capability for thermal and cold neutrons together with correlated high position sensitive readout and up to 100 MHz for individual single pixel readout.

## 7. Summary

The CASCADE detector is designed for neutron applications of high intensities and high demands on the dynamical range, contrast as well as background. It combines technology from high-energy physics research with the specialized and particular necessities in neutron research. The system conceptually is targeted for self-sufficient autarkic operation with asynchronous data transfer for analysis. The actual detector configuration has a spatial resolution of 2.6 mm (FWHM). Operated at ambient pressure it is a lightweight cubical module, exposing a sensitive area of 200mm × 200mm with a blind area of 10 mm width including its housing. Several of these can be tiled to build up multi-detector setups. In the current configuration, each module is capable of detecting a maximum of  $10^6$  neutrons/s at ten percent dead time, limited only by the correlated readout strategy employed. The detector can cope with SNS/J-PARC-type source intensities and it can exploit their time structure. In

respect to the severe crisis in supply of  $^3\text{He}$ , CASCADE has evolved to be a technological alternative to  $^3\text{He}$  based neutron detectors.

Finally, the system lends itself for customization towards a modified set of specifications in terms of rate capability, size or resolution or other incremental future improvements. It can be easily adapted to special neutron applications. First adapted prototypes have been build and successfully tested for resolving very fast neutron intensity modulations in MIEZE applications, higher position resolution with higher gas pressure and as a beam monitor detector.

## Acknowledgements

We cordially thank D. Dubbers (university of Heidelberg) for his steady encouragement on this work and his support during the last years. We would like to thank U. Schmidt (university of Heidelberg) for all the stimulating discussions and helpful contributions. We are grateful also to A. Oed for his introduction into neutron detection and his stimulating enthusiasm. We would also like to thank P. Geltenbort for his support through many beam times at the ILL. This work was funded by the German Federal Ministry for Research and Education under contracts no. 03DU03HD and no. 06HD187.

- [1] T. Unruh et al., Nucl. Instr. and Meth. A 580 (2007) 1414.
- [2] B. Yu et al., Nucl. Instr. and Meth. A 513 (2003) 362.
- [3] R. Kampmann et al., Nucl. Instr. and Meth. A 529 (2004) 342.
- [4] R. G. Cooper, Nucl. Instr. and Meth. A 529 (2004) 394.
- [5] Y. Fujii, Nucl. Instr. and Meth. A 529 (2004) 1.
- [6] J. C. Buffet, Nucl. Instr. and Meth. A 554 (2005) 392.
- [7] "Helium-3 shortage could put freeze on low-temperature research", Science, Vol. 326, 06.11.2009, p. 778.
- [8] F. Sauli, Nucl. Instr. and Meth. A 386 (1997) 531.
- [9] A. Bressan et. al., Nucl. Instr. and Meth. A 425 (1999) 262.
- [10] M. Villa et. al., paper presented at this Conference.
- [11] A. Bressan et. al., Nucl. Instr. and Meth. A 425 (1999) 254.
- [12] C. Lundstedt et al., Nucl. Instr. and Meth. A 562 (2006) 380.
- [13] D. S. McGregor et al., Nucl. Instr. and Meth. A 591 (2008) 530.
- [14] M. Schieber et al., Nucl. Instr. and Meth. A 579 (2007) 180.
- [15] B. Gebauer et. al., Nucl. Instr. and Meth. A 529 (2004) 358.
- [16] T. C. Unruh et al., Nucl. Instr. and Meth. A 604 (2009) 150.
- [17] N. J. Rhodes et al., Nucl. Instr. and Meth. A 529 (2004) 243.
- [18] A. S. Tremsin et al., paper presented at this Conference.
- [19] D.S. McGregor et. al., Nucl. Instr. and Meth. A 500 (2003) 272.
- [20] M. Klein, "Experimente zur Quantenmechanik mit ultrakalten Neutronen und Entwicklung eines neuen Detektors zum orts aufgelösten Nachweis von thermischen Neutronen auf großen Flächen", PhD-thesis (2000), University of Heidelberg.
- [21] J. Becker et. al., Nucl. Instr. and Meth. A 586 (2008) 190.
- [22] H. Abele et al., Nucl. Instr. and Meth. A 562 (2006) 407.
- [23] R. Golub et al., Am. J. Phys. 62 (9) (1994) 779.
- [24] C. J. Schmidt et. al., "CASCADE with NRSE: Fast Intensity Modulation Techniques used in Quasielastic Neutron Scattering", Journal of Physics, accepted to be published.
- [25] A. S. Brogna et. al., Nucl. Instr. and Meth. A 568 (2006) 301.